



Development and validation of a glioma prognostic model based on telomere-related genes and immune infiltration analysis

Xiaozhuo Liu¹, Jingjing Wang², Dongpo Su³, Qing Wang¹, Mei Li¹, Zhengyao Zuo¹, Qian Han¹, Xin Li¹, Fameng Zhen¹, Mingming Fan¹, Tong Chen¹

¹Department of Neurosurgery, Affiliated Hospital of North China University of Science and Technology, Tangshan, China; ²Department of Imaging, Affiliated Hospital of North China University of Science and Technology, Tangshan, China; ³School of Clinical Medicine, Ningxia Medical University, Yinchuan, China

Contributions: (I) Conception and design: X Liu, T Chen; (II) Administrative support: T Chen; (III) Provision of study materials or patients: J Wang, D Su; (IV) Collection and assembly of data: Q Wang, M Li, Z Zuo, Q Han; (V) Data analysis and interpretation: X Li, F Zhen, M Fan; (VI) Manuscript writing: All authors; (VII) Final approval of manuscript: All authors.

Correspondence to: Tong Chen, MD. Department of Neurosurgery, Affiliated Hospital of North China University of Science and Technology, No. 73, Jianshe South Road, Lubei District, Tangshan 063000, China. Email: ct.1973@163.com.

Background: Gliomas are the most prevalent primary brain tumors, and patients typically exhibit poor prognoses. Increasing evidence suggests that telomere maintenance mechanisms play a crucial role in glioma development. However, the prognostic value of telomere-related genes in glioma remains uncertain. This study aimed to construct a prognostic model of telomere-related genes and further elucidate the potential association between the two.

Methods: We acquired RNA-seq data for low-grade glioma (LGG) and glioblastoma (GBM), along with corresponding clinical information from The Cancer Genome Atlas (TCGA) database, and normal brain tissue data from the Genotype-Tissue Expression (GTEx) database for differential analysis. Telomere-related genes were obtained from TelNet. Initially, we conducted a differential analysis on TCGA and GTEx data to identify differentially expressed telomere-related genes, followed by Gene Ontology (GO) and Kyoto Encyclopedia of Genes and Genomes (KEGG) enrichment analyses on these genes. Subsequently, univariate Cox analysis and log-rank tests were employed to obtain prognosis-related genes. Least absolute shrinkage and selection operator (LASSO) regression analysis and multivariate Cox regression analysis were sequentially utilized to construct prognostic models. The model's robustness was demonstrated using receiver operating characteristic (ROC) curve analysis, and multivariate Cox regression of risk scores for clinical characteristics and prognostic models were calculated to assess independent prognostic factors. The aforementioned results were validated using the Chinese Glioma Genome Atlas (CGGA) dataset. Finally, the CIBERSORT algorithm analyzed differences in immune cell infiltration levels between high- and low-risk groups, and candidate genes were validated in the Human Protein Atlas (HPA) database.

Results: Differential analysis yielded 496 differentially expressed telomere-related genes. GO and KEGG pathway analyses indicated that these genes were primarily involved in telomere-related biological processes and pathways. Subsequently, a prognostic model comprising ten telomere-related genes was constructed through univariate Cox regression analysis, log-rank test, LASSO regression analysis, and multivariate Cox regression analysis. Patients were stratified into high-risk and low-risk groups based on risk scores. Kaplan-Meier (K-M) survival analysis revealed worse outcomes in the high-risk group compared to the low-risk group, and establishing that this prognostic model was a significant independent prognostic factor for glioma patients. Lastly, immune infiltration analysis was conducted, uncovering notable differences in the proportion of multiple immune cell infiltrations between high- and low-risk groups, and eight candidate genes were verified in the HPA database.

Conclusions: This study successfully constructed a prognostic model of telomere-related genes, which can more accurately predict glioma patient prognosis, offer potential targets and a theoretical basis for glioma treatment, and serve as a reference for immunotherapy through immune infiltration analysis.

Keywords: Bioinformatics; glioma; immune infiltration; prognosis; telomere

Submitted Dec 13, 2023. Accepted for publication Jun 04, 2024. Published online Jul 22, 2024.

doi: 10.21037/tcr-23-2294

View this article at: <https://dx.doi.org/10.21037/tcr-23-2294>

Introduction

Gliomas represent the most prevalent malignant tumors in the central nervous system and are classified by the World Health Organization as low-grade gliomas (LGGs) and high-grade gliomas (HGGs). Although LGGs exhibit a more favorable prognosis compared to HGGs, treatment resistance and tumor recurrence remain inevitable following a combination of surgery, radiotherapy, and chemotherapy. Consequently, over half of the patients will ultimately develop highly aggressive gliomas (1-3). Glioblastoma (GBM) is the most common and aggressive grade IV glioma, characterized by the highest malignancy, poorest prognosis, and lowest overall survival rate. The

median survival time for GBM patients is approximately fifteen months, with a five-year survival rate of about 7.2% (4,5). Despite comprehensive multimodal treatment approaches, significant breakthroughs remain elusive, primarily due to factors such as tumor heterogeneity, tumor microenvironment, and the blood-brain barrier. Thus, a comprehensive understanding of the molecular mechanisms underlying glioma development will provide novel theoretical foundations and insights for glioma diagnosis, treatment, and prognosis.

Human telomeres are located at the ends of chromosomes and consist of DNA repetitive sequences (TTAGGG) and several related telomere-binding proteins (6). Cell division results in telomere shortening, and when telomere length falls below a critical threshold, cells undergo senescence and apoptosis (7). However, cancer cells can circumvent progressive telomere shortening and activate telomere maintenance mechanisms (TMM) to preserve telomere length (8). Currently, two TMMs have been identified in cancer research: the most common mechanism, telomerase activation (9), and the alternative lengthening of telomeres (ALT) mechanism, which does not rely on telomerase to extend telomeres (10). Studies have indicated that TMM activity in osteosarcoma and neuroblastoma may exhibit intratumor heterogeneity, with ALT and telomerase functioning in different cells within the same tumor (11,12).

Gliomas have a strong association with TMM, and alterations in telomerase reverse transcriptase (*TERT*), specifically *TERT* promoter (*TERT*_p) mutations, are considered the primary mechanism of telomerase activation in both GBM and LGG (13-15). ALT is typically observed in World Health Organization (WHO) grade II or III isocitrate dehydrogenase (IDH)-mutated astrocytomas and IDH-mutated GBMs (16), and abnormalities in the *ATRX/DAXX/H3.3* complex have been found to be closely related to the ALT mechanism (17). Based on these findings, it is evident that TMM plays a significant role in glioma development; however, the prognostic role of telomere-related genes in glioma remains unclear. Therefore, in this study, we aimed to construct a prognostic model of telomere-related genes in glioma to provide novel research

Highlight box

Key findings

- We constructed prognostic models with ten telomere-related genes (*GANAB*, *PPP1R1B*, *CDC73*, *IGF2BP3*, *FEN1*, *RMI2*, *HNRNPA0*, *ANXA2*, *LCK*, *ZGPAT*) and validated eight of them in the Human Protein Atlas (HPA) database.
- Three R packages for analysis of differences were used to take the intersection of the results; and the prognostic analysis of the difference genes was performed by univariate Cox analysis and log-rank tests, which increased the reliability of the prognostic model genes.
- The study showed that the abnormal expression of telomere related genes has a significant effect on the prognosis of glioma patients, which provides reference for the treatment of glioma by telomere targets.

What is known and what is new?

- Increasing evidence suggests that telomere maintenance mechanisms play a crucial role in glioma development.
- This study aimed to construct a prognostic model of telomere-related genes and further elucidate the potential association between the two.

What is the implication, and what should change now?

- This study successfully constructed a prognostic model of telomere-related genes, which can more accurately predict glioma patient prognosis, offer potential targets and a theoretical basis for glioma treatment, and serve as a reference for immunotherapy through immune infiltration analysis.

targets and insights for telomere-related therapy in glioma management. We present this article in accordance with the TRIPOD reporting checklist (available at <https://tcr.amegroupp.com/article/view/10.21037/tcr-23-2294/rc>).

Methods

Data collection and processing

RNA-seq data and clinical follow-up information for LGG and GBM were obtained from The Cancer Genome Atlas (TCGA) database (<https://portal.gdc.cancer.gov/>). Cases with unknown survival dates or life and death statuses were excluded, resulting in a total of 664 cases for the training set. Similarly, RNA-seq data and corresponding clinical information for the Chinese Glioma Genome Atlas (CGGA) cohorts (mRNAseq_693, mRNAseq_325) were acquired from the CGGA database (<http://www.cgga.org.cn>) as the validation set. Moreover, 1,148 normal brain samples were procured from the Genotype-Tissue Expression (GTEx) database via the UCSC Xena website (<https://xenabrowser.net/datapages/>) for differential analysis. Telomere-associated genes were sourced from www.cancertelsys.org/telnet (18). Batch effects were removed using the limma package. This study was conducted in accordance with the Declaration of Helsinki (as revised in 2013).

Differential expression and functional enrichment analysis

By integrating the RNA-seq data for LGG and GBM from the TCGA database with the 1,148 normal brain samples from the GTEx database on the UCSC XENA website, we conducted a differential analysis using the DESeq2, limma, and edgeR packages, with a threshold at $P < 0.05$ and $|\log_2(\text{fold change})| > 1$. Overlapping differentially expressed genes were identified using Venn diagrams for subsequent analysis. Additionally, we intersected telomere-related genes with the differentially expressed genes. The ClusterProfiler R package was then employed for Gene Ontology (GO) and Kyoto Encyclopedia of Genes and Genomes (KEGG) enrichment analyses (19,20), with an adjusted P value threshold of < 0.05 .

Construction of telomere-related gene risk model

To construct a risk model for telomere-related genes, we performed univariate Cox regression analysis, log-rank test, least absolute shrinkage and selection operator (LASSO)

regression analysis, and multivariate Cox regression analysis on telomere-associated differentially expressed genes. Genes with a P value < 0.05 were deemed to have significant prognostic value, resulting in the identification of 10 prognostic-associated genes. We then calculated the risk score using the formula: risk score = gene expression level 1 $\times \beta_1$ + gene expression level 2 $\times \beta_2$ + ... + gene expression level n $\times \beta_n$, where β is the regression coefficient for each gene determined by multivariate Cox regression. Based on median risk scores, patients were stratified into high-risk and low-risk groups. The relationship between risk groups and overall survival (OS) was assessed through Kaplan-Meier (K-M) survival analysis, and the accuracy of predicting patient outcomes at 1, 3, and 5 years was evaluated using receiver operating characteristic (ROC) curves with the timeROC R package.

Assessment of independent prognostic factors and construction of nomogram

We conducted a multivariate Cox regression analysis, incorporating risk scores and clinicopathological characteristics (e.g., sex, age), to determine if telomere-related risk models could serve as independent prognostic factors. A nomogram was subsequently constructed using the rms R package (21).

Immune infiltration analysis

CIBERSORT (22) is a method for estimating and analyzing immune cell infiltration based on the principle of deconvolution. We employed CIBERSORT to estimate the proportions of immune cell types in the low-risk and high-risk groups, setting the number of permutations to 1,000 and using a P value threshold of < 0.05 for screening.

Immunohistochemistry

To validate the expression of candidate genes in the prognostic models for gliomas, we obtained immunohistochemical images of protein-level expression for eight prognostic genes in normal brain tissue and glioma tissue from the Human Protein Atlas (HPA) (www.proteinatlas.org).

Statistical analysis

Statistical analyses and chart generation were conducted

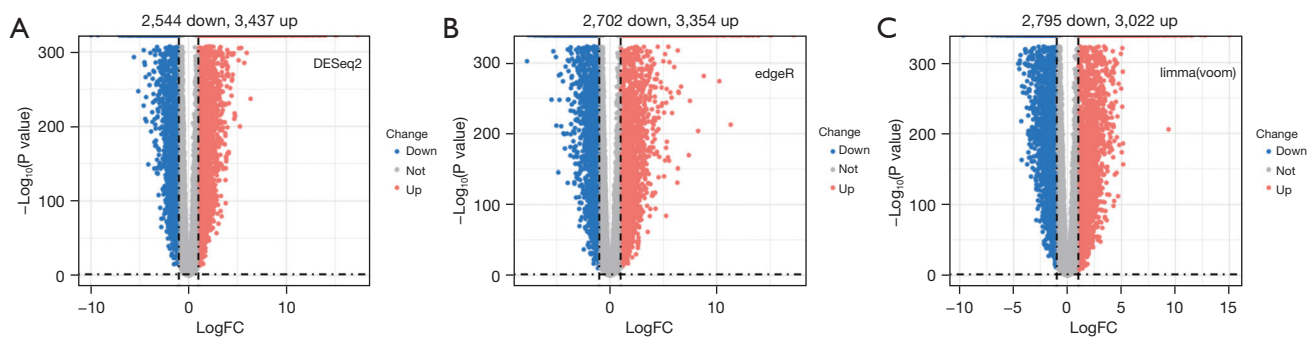


Figure 1 Volcano plots of differentially expressed genes between glioma and normal brain tissue. (A) DESeq2 differential analysis volcano plot; (B) edgeR differential analysis volcano plot; (C) limma differential analysis volcano plot. Red dots represent upregulated genes and blue dots represent downregulated genes. FC, fold change.

using R software (version 4.1.3). The R package “survival” was utilized for univariate and multivariate Cox regression analyses to evaluate prognostic value; the R package “survminer” was employed for Kaplan-Meier survival analysis to estimate OS between patient groups; the R package “rms” was used for creating nomograms and calibration curves; and the R package “timeROC” was used for generating ROC curves to assess the accuracy of patient outcome predictions. A P value <0.05 was considered statistically significant.

Results

Identification of telomere-related differentially expressed genes in glioma patients and enrichment analysis

We integrated glioma patient samples with normal brain tissue samples and assessed the differences using the DESeq2, limma, and edgeR packages, respectively (Figure 1A-1C), applying thresholds of $P < 0.05$ and $|\log FC| > 1$. We then identified overlapping differentially expressed genes through a Venn diagram, resulting in a total of 2,318 downregulated and 2,836 upregulated differentially expressed genes (Figure 2A,2B). By intersecting the 2,086 telomere-related genes acquired from TelNet with the aforementioned differentially expressed genes and requiring gene expression levels to be greater than 0 in at least 350 samples, we ultimately obtained 214 upregulated and 282 downregulated genes. Furthermore, we conducted functional enrichment analysis of the telomere-related differentially expressed genes. In the GO enrichment analysis, biological processes (BP) (Figure 3A) were primarily linked to DNA recombination and replication, DNA

conformational change, telomere maintenance, regulation of DNA biosynthesis process, and negative regulation of cell cycle process. Cellular components (CC) (Figure 3B) were predominantly associated with chromosome (telomeric region) and DNA replication preinitiation complex, while molecular functions (MF) (Figure 3C) were chiefly related to catalytic activity acting on DNA, protein serine/threonine kinase activity, ATP hydrolysis activity, and telomeric DNA binding. The KEGG enrichment analysis (Figure 3D) indicated that the main pathways involved were DNA replication, cell cycle, homologous recombination, cellular senescence, and calcium signaling pathway.

Construction and validation of a prognostic model for telomere-related genes

A total of 496 differentially expressed genes were subjected to univariate Cox regression and log-rank test analyses, resulting in the identification of 372 genes associated with glioma prognosis. To validate these prognostic genes in the CGGA-693 and CGGA-325 datasets, univariate Cox regression and log-rank test analyses were performed on both datasets, and the prognostic genes from all three datasets were intersected, yielding 252 genes. To avoid overfitting and enhance prediction accuracy, the 252 prognostic genes were subjected to LASSO regression analysis. With an optimal λ value of 0.01033, 43 genes were obtained for further investigation (Figure 4A,4B). Ultimately, 10 genes significantly linked to poor prognosis were identified through multivariate Cox regression analysis (Figure 5). In Figure 5, GANAB, PPP1R1B, IGF2BP3, RMI2 and ANXA2 are located on the right side of the invalid line, with HR >1, indicating that glioma

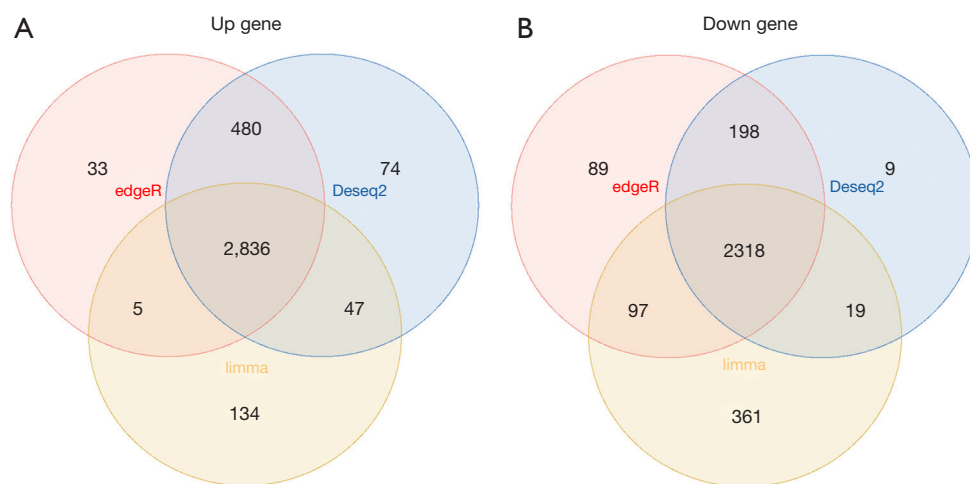


Figure 2 Venn diagram of differential genes. (A) Venn diagram of expressed up-regulated genes obtained from three differential analysis R packages; (B) Venn diagram of expressed down-regulated genes obtained from three differential analysis R packages.

patients have increased expression levels of these genes compared with normal population, suggesting poor prognosis and belonging to risk factors. CDC73, FEN1 and HNRNPA0 were located on the left side of the null line, with HR <1, indicating that glioma patients had lower expression levels of these genes compared with the normal population, indicating poor prognosis and belonging to protective factors. The risk score for each patient was calculated using the formula [risk score = $GANAB \times 1.32108 + PPP1R1B \times 0.14476 + CDC73 \times (-0.84312) + IGF2BP3 \times 0.18173 + FEN1 \times (-0.53136) + RMI2 \times 0.54494 + HNRNPA0 \times (-0.95043) + ANXA2 \times 0.25578 + LCK \times (-0.08713) + ZGPAT \times 0.08506$]. Patients were then classified into high-risk and low-risk groups based on median risk score values. Kaplan-Meier survival analysis was performed on both patient groups, revealing that the OS was significantly higher in the low-risk group compared to the high-risk group in the TCGA dataset, CGGA-693 dataset, and CGGA-325 dataset (Figure 6A-6C). The difference in survival curves between the low-risk and high-risk groups was statistically significant ($P < 0.001$). Furthermore, the distribution of risk scores, survival status, and risk gene expression for the TCGA cohort and the two validation cohorts are depicted in the figure (Figure 7A-7C).

Utilization of telomere-related risk scores as independent prognostic factors and construction of a nomogram

To determine whether telomere-related risk scores can

function as an independent predictor of OS in patients, we incorporated age, gender, and risk score into a multivariate Cox regression analysis. The findings demonstrated that both risk score and age were independent prognostic factors for glioma patients (Figure 8A-8C). Subsequently, we evaluated the sensitivity and specificity of this prognostic model using time-dependent ROC curves. The 1-, 3-, and 5-year area under the curve (AUC) values for the TCGA cohort (Figure 9A) were 0.878, 0.920, and 0.902, respectively. For the CGGA-693 cohort (Figure 9B), the 1-year, 3-year, and 5-year AUC values were 0.768, 0.822, and 0.839, respectively, while for the CGGA-325 cohort (Figure 9C), they were 0.795, 0.866, and 0.899, respectively. These results indicate strong predictive performance. We subsequently constructed a nomogram (Figure 10), and calibration curves at 1, 3, and 5 years revealed the nomogram accurately predicted the survival time of patients in the TCGA cohort (Figure 11A). Similar results were observed in the CGGA-693 and CGGA-325 cohorts (Figure 11B,11C).

Immune infiltration analysis

We employed the CIBERSORT algorithm to assess the differences in immune cell proportions between high-risk and low-risk groups in the TCGA cohort. Notably, the high-risk group exhibited increased proportions of T cells CD4 memory resting, NK cells resting, NK cells activated, macrophages M1, macrophages M2, mast cells resting, and neutrophils compared to the low-risk group. In contrast, the

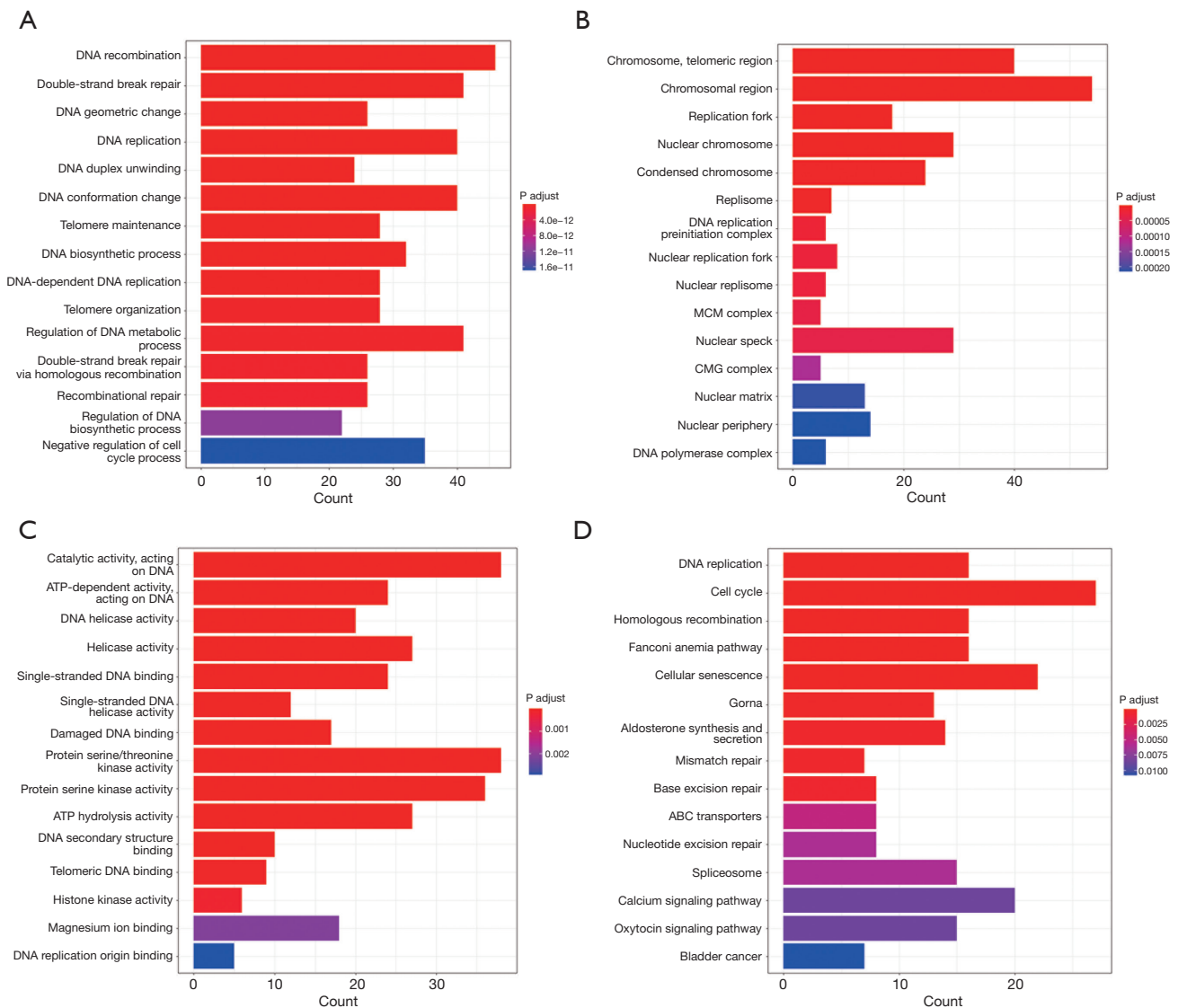


Figure 3 GO and KEGG functional enrichment analysis. (A) Top 15 terms of BP in GO; (B) top 15 terms of CC in GO; (C) top 15 terms of MF in GO; (D) top 15 pathways of KEGG enrichment analysis. The length of the horizontal bar in the figure indicates the number of genes, and the color change of the horizontal bar represents different P values. GO, Gene Ontology; KEGG, Kyoto Encyclopedia of Genes and Genomes; BP, biological processes; CC, cellular components; MF, molecular functions.

high-risk group demonstrated lower proportions of B cells naïve, plasma cells, T cells CD4 naïve, T cells regulatory (Tregs), T cells gamma delta, dendritic cells resting, mast cells activated, and eosinophils (Figure 12).

Immunohistochemistry

To validate protein-level expression in normal brain tissue and glioma tissue, we examined *GANAB* (Figure 13A,13B),

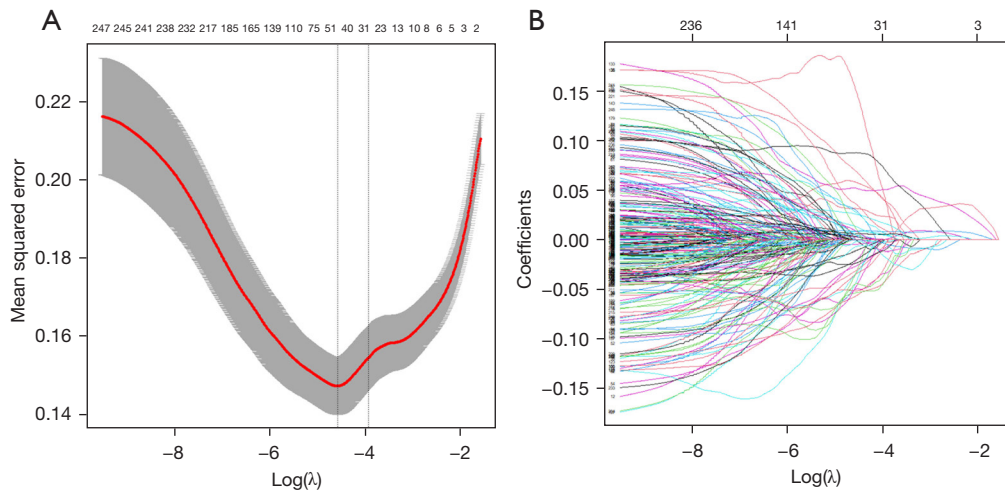


Figure 4 LASSO regression analysis. (A) Cross-validation for tuning parameter selection in the LASSO regression model; (B) LASSO coefficient profiles. LASSO, least absolute shrinkage and selection operator.

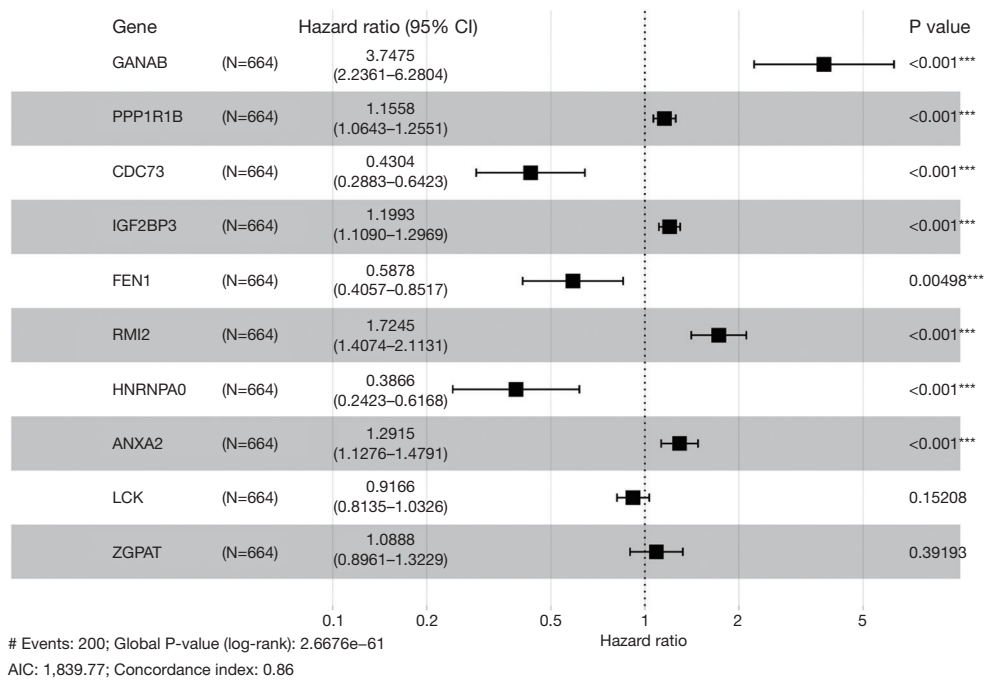


Figure 5 Forest plot. Ten telomere related prognostic genes were screened using multivariate Cox regression analysis to construct a prognostic model. ***, P<0.001. CI, confidence interval; AIC, Akaike information criterion.

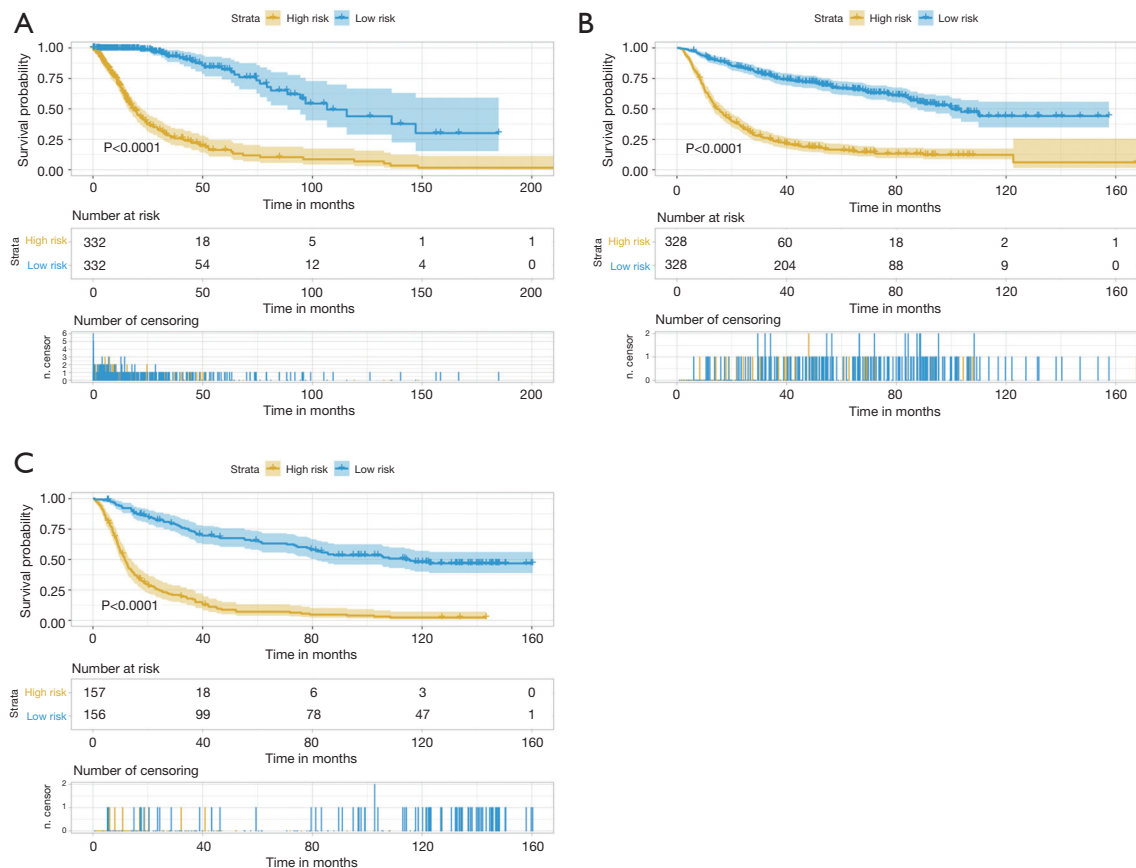


Figure 6 Kaplan-Meier survival curve plot. (A-C) Kaplan-Meier curves for survival status and survival time of TCGA cohort, CGGA-693 cohort and CGGA-325 cohort. The yellow curve represents the high-risk group and the blue curve represents the low-risk group. TCGA, The Cancer Genome Atlas; CGGA, the Chinese Glioma Genome Atlas.

PPP1R1B (Figure 13C,13D), *CDC73* (Figure 14A,14B), *IGF2BP3* (Figure 14C,14D), *FEN1* (Figure 15A,15B), *RMI2* (Figure 15C,15D), *HNRNPA0* (Figure 16A,16B), and *ANXA2* (Figure 16C,16D) using the HPA database for immunohistochemical analysis.

Discussion

Gliomas represent approximately 30% of primary brain tumors and 80% of malignant brain tumors, with their pathogenesis remaining unclear (23). Fluorescence-guided techniques have been employed to enhance tumor resection rates (24,25), and a combination of multiple modalities, including radiotherapy, immunotherapy, targeted therapy,

and tumor electric field therapy, has been utilized (26). However, these approaches have not significantly improved the survival and prognosis of patients with high-grade gliomas. The release of the fifth edition of the World Health Organization Classification of Tumors of the Central Nervous System (WHO CNS5) (27) emphasized the importance of molecular markers in classifying CNS tumors, thereby providing a foundation for precise treatment.

Research has demonstrated that TMM can grant cancer cells the ability to proliferate indefinitely and inhibit senescence (28). In glioma, the telomerase activation mechanism and the ALT mechanism are particularly significant. Nonetheless, the impact of telomere-related

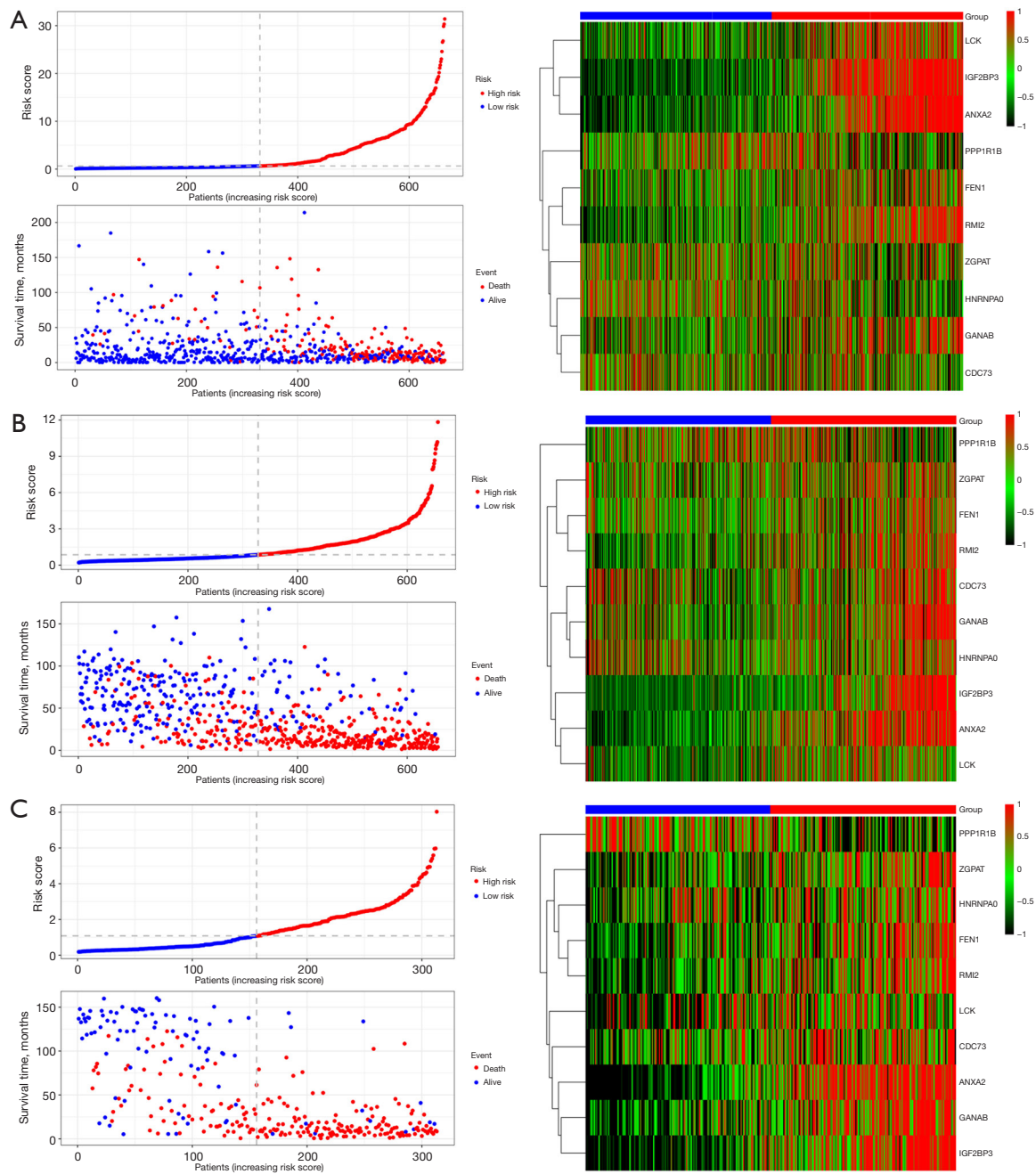


Figure 7 Distribution plots. (A-C) Distribution of risk scores and survival status in the TCGA cohort, CGGA-693 cohort and CGGA-325 cohort, and heat map of 10 prognostic genes expressed in the high and low risk groups. Red dots indicate dead, blue dots indicate alive. TCGA, The Cancer Genome Atlas; CGGA, the Chinese Glioma Genome Atlas.

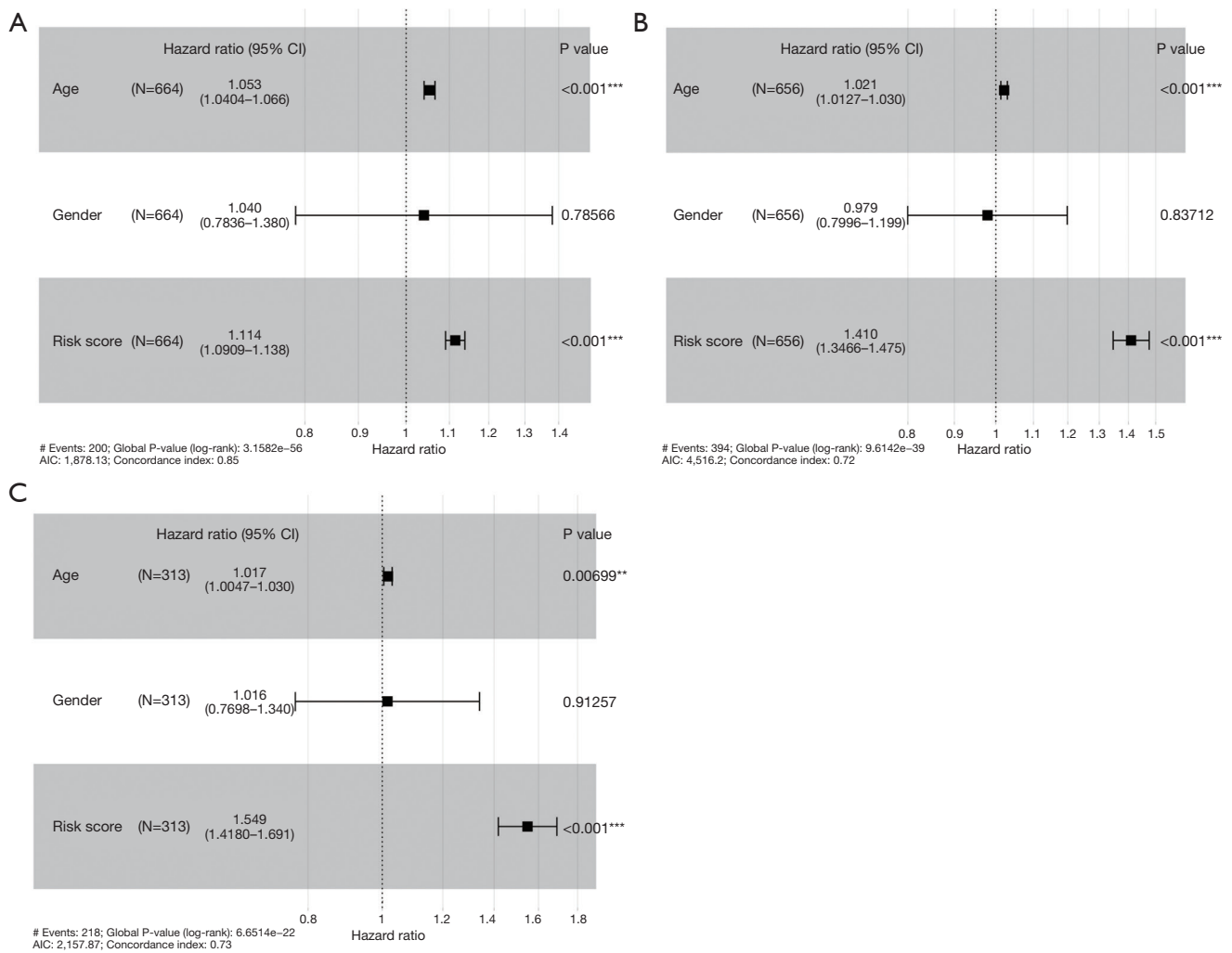


Figure 8 To validate the clinical independence of telomere related prognostic features in the TCGA and CGGA cohorts. (A-C) Multivariate Cox regression analysis for the TCGA cohort, CGGA-693 cohort and CGGA-325 cohort for assessing independent prognostic factors. ***, P<0.001; **, P<0.01. CI, confidence interval; AIC, Akaike information criterion; TCGA, The Cancer Genome Atlas; CGGA, the Chinese Glioma Genome Atlas.

genes on glioma remains inadequately understood. Consequently, this study aimed to identify differentially expressed telomere-related genes within glioma datasets and construct a prognostic model. This model may offer insights for discovering tumor molecular markers to evaluate prognostic effects and identify potential drug targets for inhibiting glioma proliferation.

In this study, we analyzed glioma sequencing data and corresponding clinical data from the TCGA and CGGA databases, identifying 496 differentially expressed telomere-related genes, including 214 upregulated and 282 downregulated genes. GO and KEGG enrichment

analyses revealed that these genes were closely associated with DNA replication, telomere maintenance, and cell cycle regulation. Utilizing univariate Cox regression analysis, log-rank test, LASSO regression analysis, and multivariate Cox regression analysis, we constructed a prognostic model comprising 10 telomere-related genes (*GANAB*, *PPP1R1B*, *CDC73*, *IGF2BP3*, *FEN1*, *RMI2*, *HNRNPA0*, *ANXA2*, *LCK*, and *ZGPAT*). *IGF2BP3*, a member of the conserved *IGF2BP* family, has been demonstrated to play a crucial role in maintaining and promoting tumor heterogeneity in GBM (29). Zhang *et al.* (30) also discovered a significant positive correlation between *IGF2BP3* expression and

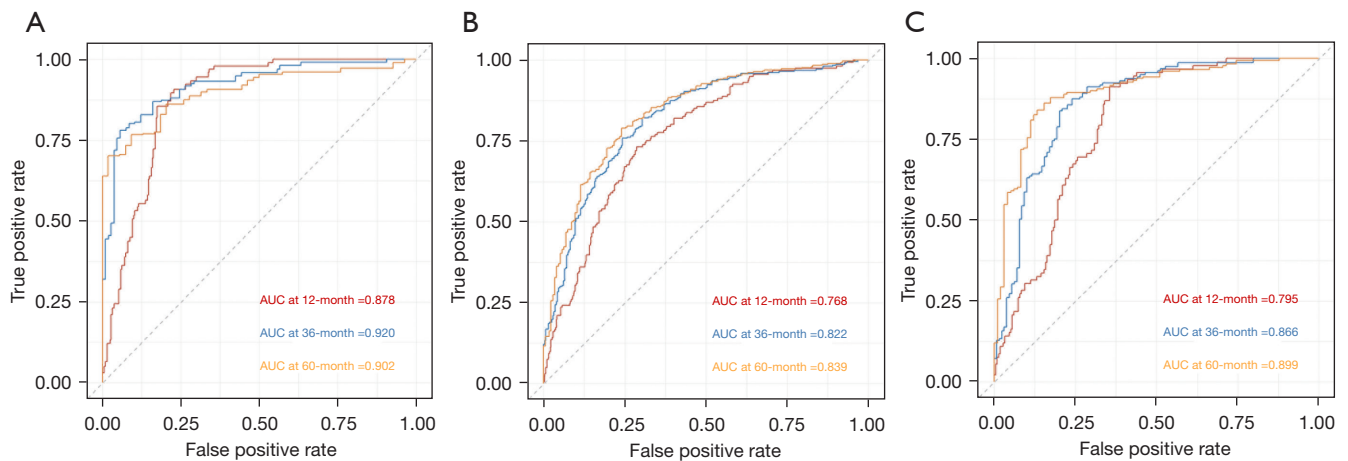


Figure 9 ROC curve analysis. (A-C) ROC curve analysis for TCGA cohort, CGGA-693 cohort and CGGA-325 cohort for validating the predictive performance of the 12-, 36- and 60-month OS risk models. AUC, area under the curve; TCGA, The Cancer Genome Atlas; CGGA, the Chinese Glioma Genome Atlas; ROC, receiver operating characteristic; OS, overall survival.

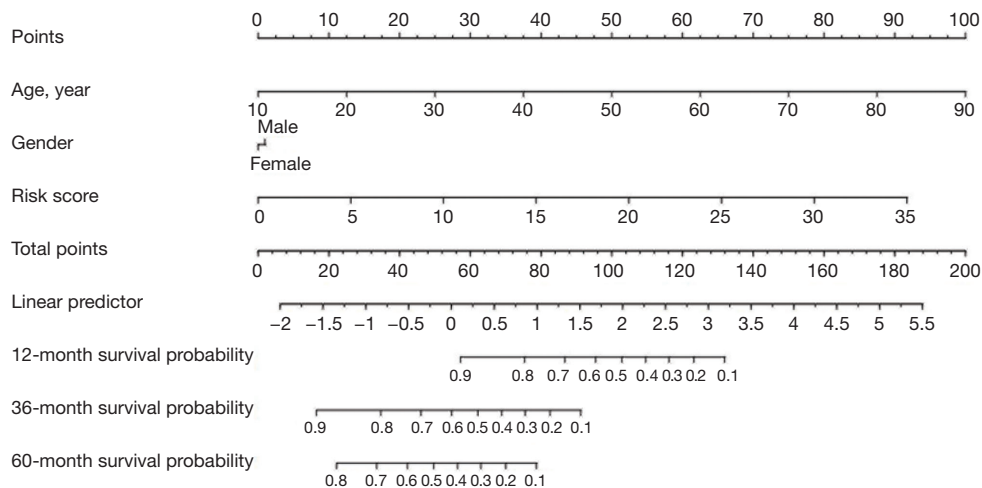


Figure 10 Nomogram. The predicted nomogram for the construction of the TCGA cohort. TCGA, The Cancer Genome Atlas.

glioma grading. *FEN1*, a structure-specific endonuclease and a typical member of the Rad2 nuclease family (31), is involved in regulatory processes such as Okazaki fragment maturation, base excision repair (BER), telomere stability maintenance, and stalled DNA replication fork repair (32). The study has shown that *FEN1* silencing can enhance cisplatin sensitivity in gliomas (33), offering potential strategies for glioma treatment. Annexin A2 (*ANXA2*), a calcium-dependent phospholipid-binding protein, has been found to be expressed on the surface of various cancer cells (34) and is implicated in numerous pathophysiological processes, including epithelial-mesenchymal transition,

tumor proliferation, migration, and cancer drug resistance (35,36). *AXNA2* is also closely related to glioma grade and poor prognosis of GBM (37), and its expression is closely associated with glioma-related inflammatory activity and immunosuppression (38). Lymphocyte-specific protein tyrosine kinase (*LCK*) is a member of the Src family (39) and plays a significant role in cell cycle control, cell adhesion, migration, and proliferation (40). Evidence suggests that *LCK*-targeted inhibitors can modulate human glioma cell migration, tumor growth, and stemness gene expression (41). Moreover, *LCK* is involved in the expansion of radiation-induced glioma-initiating cell populations

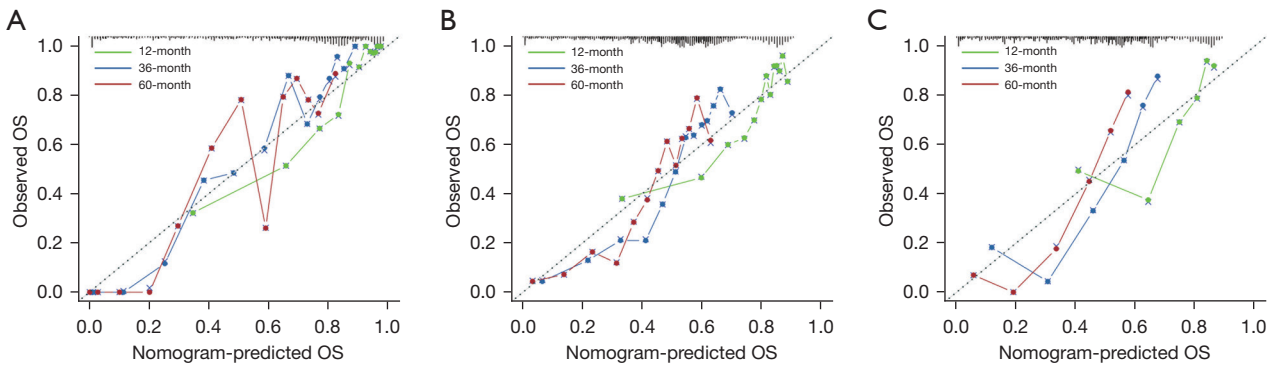


Figure 11 Calibration curve plots. (A-C) Calibration curves showing the accuracy of the TCGA cohort, CGGA693 and CGGA-325 cohort nomogram in predicting 12-, 36- and 60-month survival. OS, overall survival; TCGA, The Cancer Genome Atlas; CGGA, the Chinese Glioma Genome Atlas.

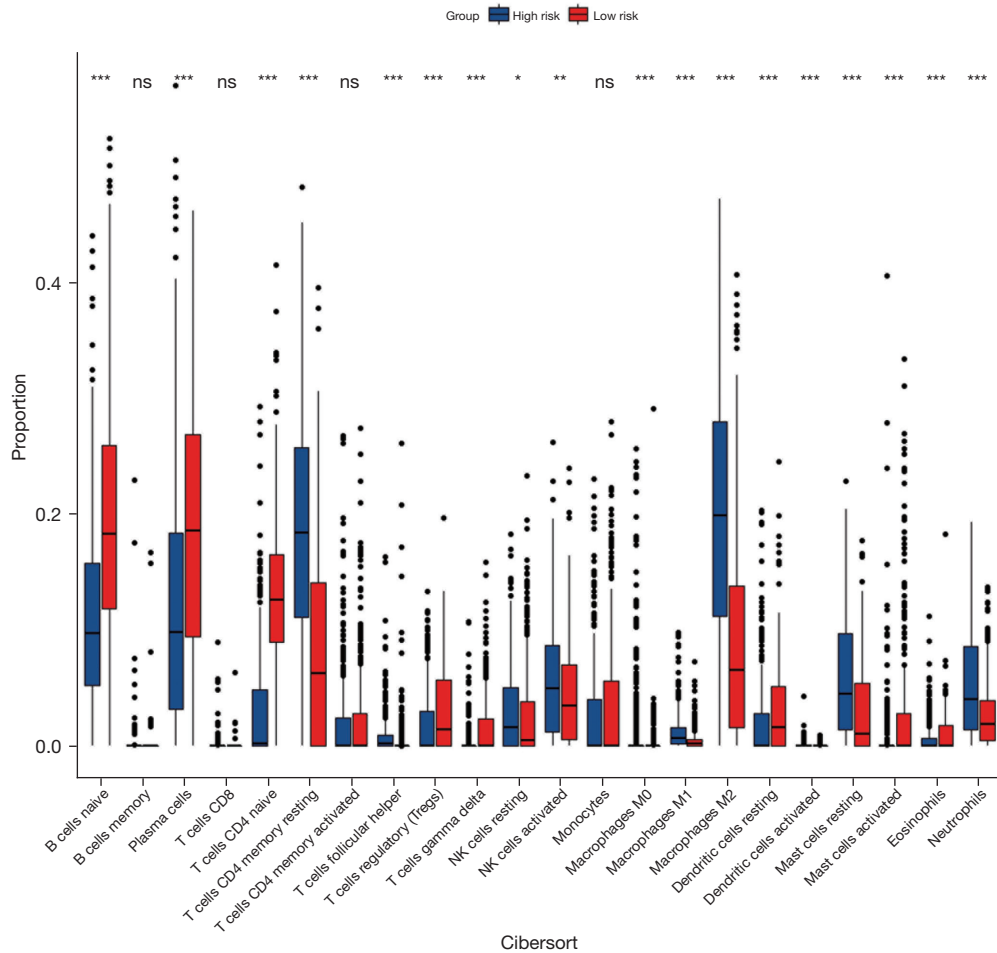


Figure 12 Boxplot for comparison of 22 immune cell fractions. Differences in the level of immune cell infiltration between the low-risk and high-risk groups. ***, $P < 0.001$; **, $P < 0.01$; *, $P < 0.05$; ns, $P \geq 0.05$.

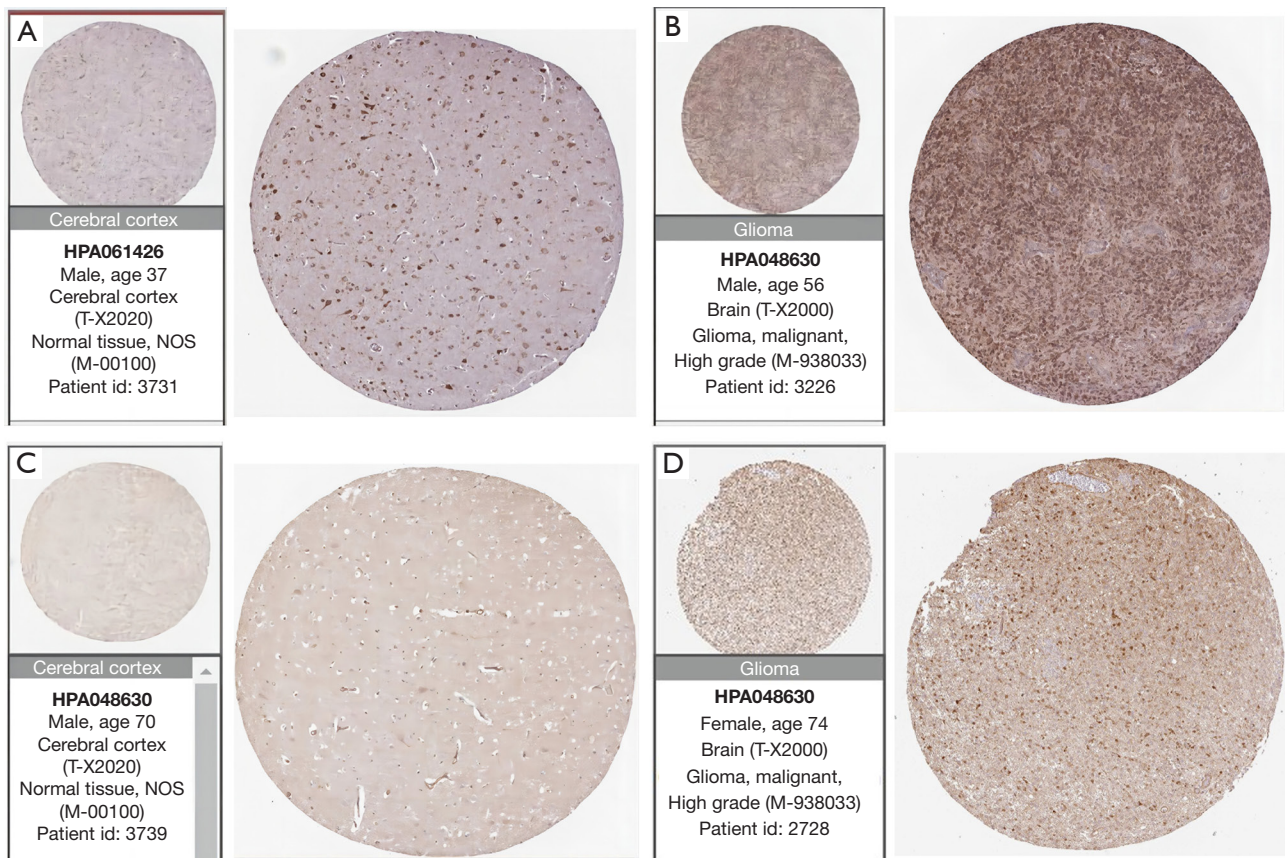


Figure 13 Immunohistochemical images. Image from the Human Protein Atlas database (<https://www.proteinatlas.org/>). (A,B) Protein expression levels of GANAB in normal cerebral cortex and glioma. The links of GANAB in normal and tumor tissues of the brain (<https://www.proteinatlas.org/ENSG00000089597-GANAB/tissue/cerebral+cortex#img>; <https://www.proteinatlas.org/ENSG00000089597-GANAB/pathology/glioma#img>). (C,D) Protein expression levels of PPP1R1B in normal cerebral cortex and glioma. The links of PPP1R1B in normal and tumor tissues of the brain (<https://www.proteinatlas.org/ENSG00000131771-PPP1R1B/tissue/cerebral+cortex#img>; <https://www.proteinatlas.org/ENSG00000131771-PPP1R1B/pathology/glioma#img>). NOS, not otherwise specified.

and contributes to decreased cell sensitivity to anticancer therapy (42). Furthermore, we stratified patients into high-risk and low-risk categories based on median risk score calculations. Kaplan-Meier survival analyses within the TCGA, CGGA-693, and CGGA-325 datasets consistently demonstrated that OS was significantly greater for the low-risk group compared to the high-risk group, with both

exhibiting statistical differences. Utilizing multivariate Cox regression analysis, we confirmed that the risk score served as an independent predictor for glioma prognosis. Subsequently, we developed a nomogram to estimate OS for glioma patients, and calibration curve validation indicated robust predictive performance. In accordance with the CIBERSORT algorithm, we observed statistically

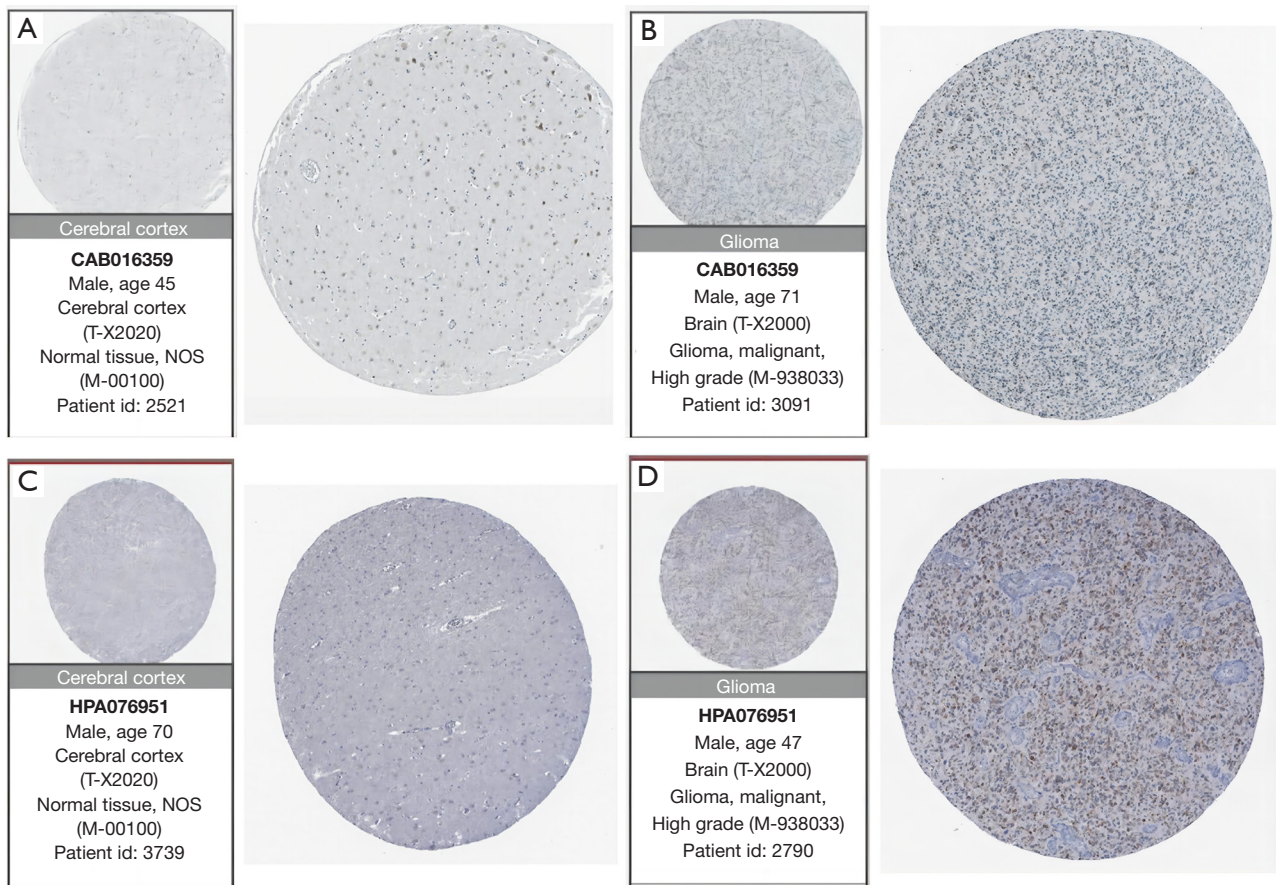


Figure 14 Immunohistochemical images. Image from the Human Protein Atlas database (<https://www.proteinatlas.org/>). (A,B) Protein expression levels of CDC73 in normal cerebral cortex and glioma. The links of CDC73 in normal and tumor tissues of the brain (<https://www.proteinatlas.org/ENSG00000134371-CDC73/tissue/cerebral+cortex#img>; <https://www.proteinatlas.org/ENSG00000134371-CDC73/pathology/glioma#img>). (C,D) Protein expression levels of IGF2BP3 in normal cerebral cortex and glioma. The links of IGF2BP3 in normal and tumor tissues of the brain (<https://www.proteinatlas.org/ENSG00000136231-IGF2BP3/tissue/cerebral+cortex#img>; <https://www.proteinatlas.org/ENSG00000136231-IGF2BP3/pathology/glioma#img>). NOS, not otherwise specified.

significant differences in the proportions of various immune cells between the high-risk and low-risk groups, offering insights for immunotherapy strategies in these distinct risk categories. Lastly, we validated eight candidate genes within the HPA database, which will facilitate the identification of reliable genes for future experimental investigations.

Conclusions

In the present investigation, we developed a glioma prognostic model centered on telomere-associated genes utilizing bioinformatics analysis, substantiating its dependability using three distinct datasets. This

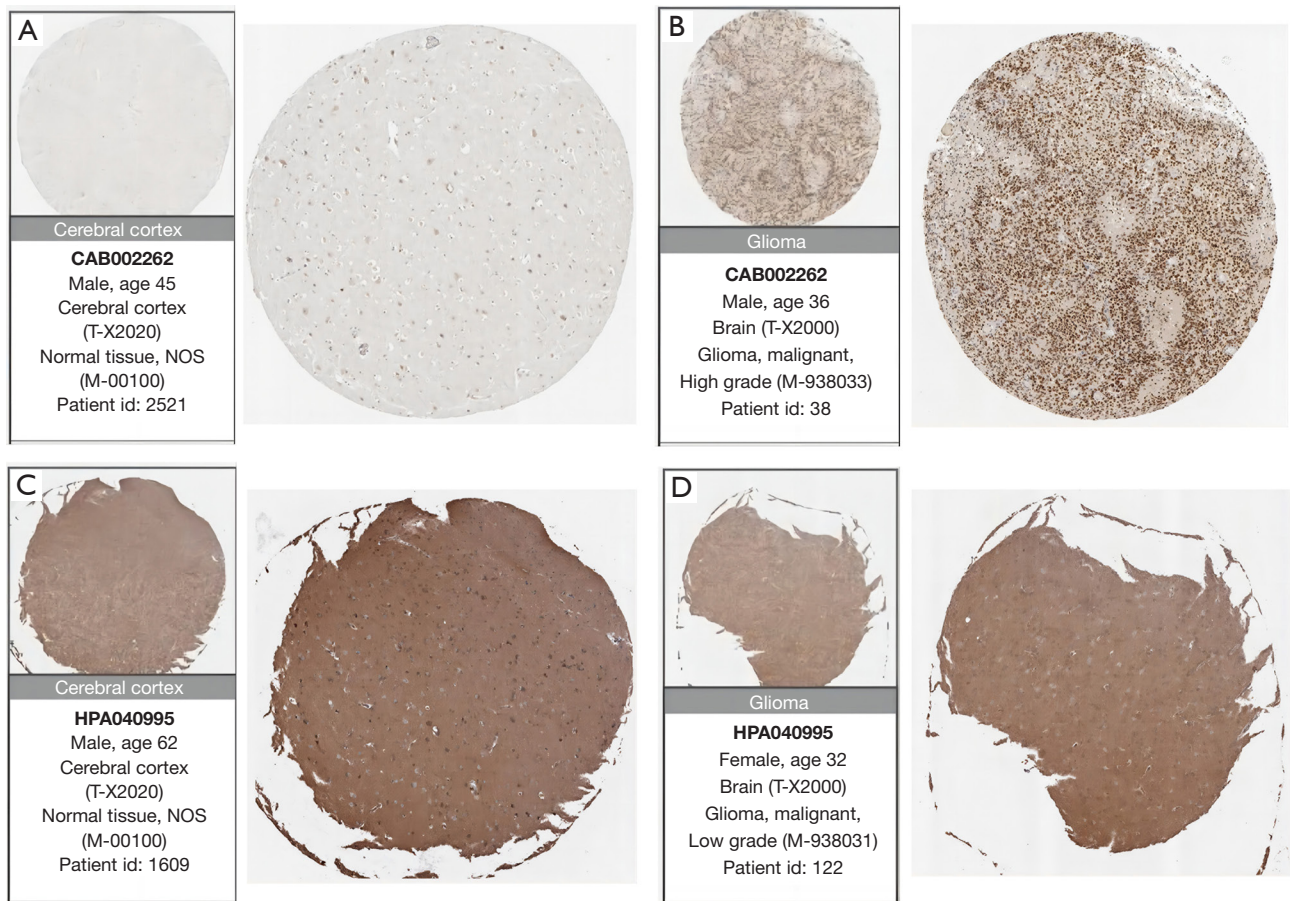


Figure 15 Immunohistochemical images. Image from the Human Protein Atlas database (<https://www.proteinatlas.org/>). (A,B) Protein expression levels of FEN1 in normal cerebral cortex and glioma. The links of FEN1 in normal and tumor tissues of the brain (<https://www.proteinatlas.org/ENSG00000168496-FEN1/tissue/cerebral+cortex#img>; <https://www.proteinatlas.org/ENSG00000168496-FEN1/pathology/glioma#img>). (C,D) Protein expression levels of RMI2 in normal cerebral cortex and glioma. The links of RMI2 in normal and tumor tissues of the brain (<https://www.proteinatlas.org/ENSG00000175643-RMI2/tissue/cerebral+cortex#img>; <https://www.proteinatlas.org/ENSG00000175643-RMI2/pathology/glioma#img>). NOS, not otherwise specified.

offers a robust foundation for clinical investigations and experimental confirmation. Despite these advancements, several limitations persist in this study. Future work will involve further validation of the identified candidate genes

and exploration of their intrinsic regulatory mechanisms through cellular and animal experimentation. Additionally, large-scale population sequencing remains necessary to corroborate the reliability of candidate genes and evaluate

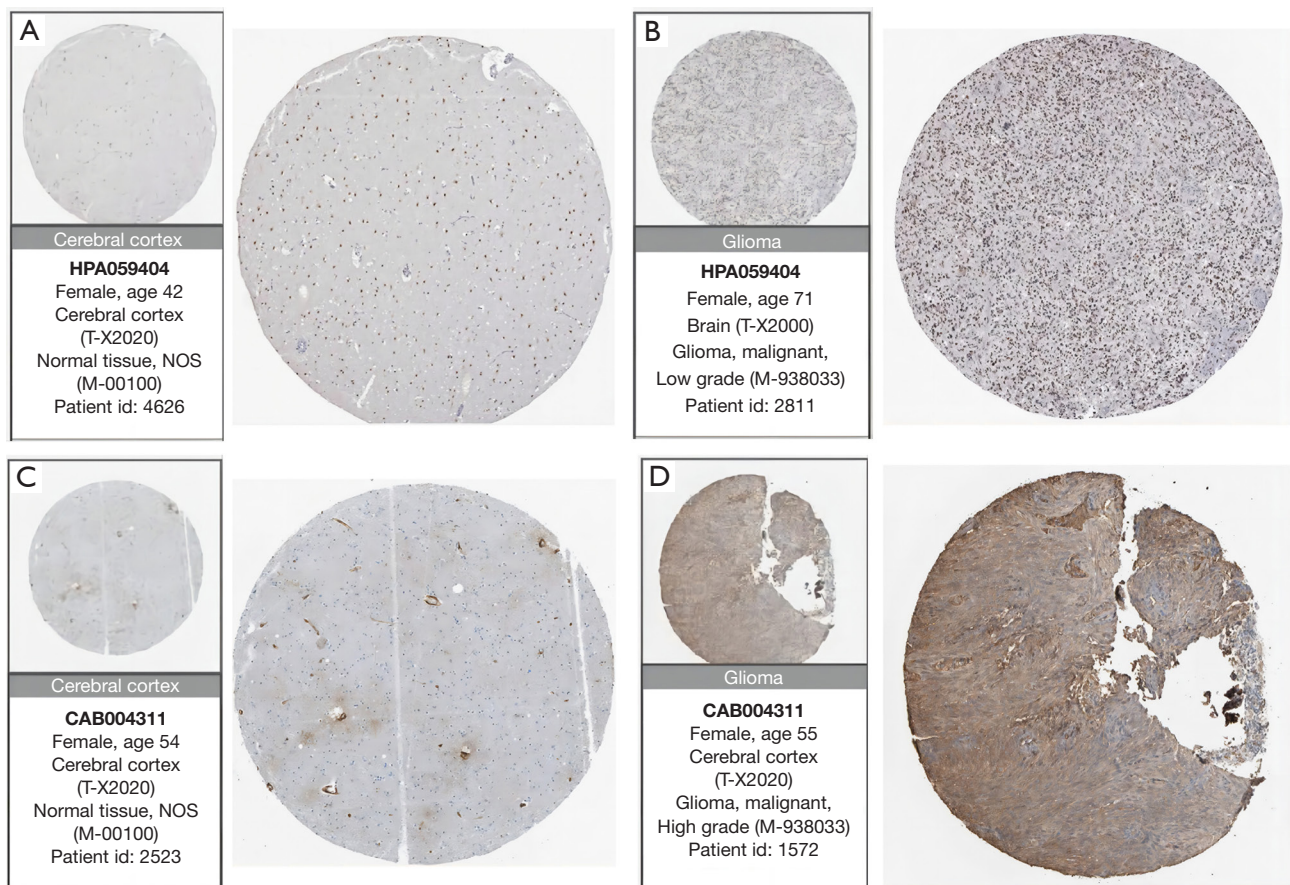


Figure 16 Immunohistochemical images. Image from the Human Protein Atlas database (<https://www.proteinatlas.org/>). (A,B) Protein expression levels of HNRNPA0 in normal cerebral cortex and glioma. The links of HNRNPA0 in normal and tumor tissues of the brain (<https://www.proteinatlas.org/ENSG00000177733-HNRNPA0/tissue/cerebral+cortex#img>; <https://www.proteinatlas.org/ENSG00000177733-HNRNPA0/pathology/glioma#img>). (C,D) Protein expression levels of ANXA2 in normal cerebral cortex and glioma. The links of ANXA2 in normal and tumor tissues of the brain (<https://www.proteinatlas.org/ENSG00000182718-ANXA2/tissue/cerebral+cortex#img>; <https://www.proteinatlas.org/ENSG00000182718-ANXA2/pathology/glioma#img>). NOS, not otherwise specified.

their potential influence on glioma patient outcomes.

Acknowledgments

We want to thank the data contributors and curators of the TCGA, GTEx, CGGA, HPA databases.

Funding: None.

Footnote

Reporting Checklist: The authors have completed the TRIPOD reporting checklist. Available at <https://tcr.amegroups.com/article/view/10.21037/tcr-23-2294/rc>

Peer Review File: Available at <https://tcr.amegroups.com/article/view/10.21037/tcr-23-2294/prf>

Conflicts of Interest: All authors have completed the ICMJE uniform disclosure form (available at <https://tcr.amegroups.com/article/view/10.21037/tcr-23-2294/coif>). The authors have no conflicts of interest to declare.

Ethical Statement: The authors are accountable for all aspects of the work in ensuring that questions related to the accuracy or integrity of any part of the work are appropriately investigated and resolved. The study was conducted in accordance with the Declaration of Helsinki (as

revised in 2013).

Open Access Statement: This is an Open Access article distributed in accordance with the Creative Commons Attribution-NonCommercial-NoDerivs 4.0 International License (CC BY-NC-ND 4.0), which permits the non-commercial replication and distribution of the article with the strict proviso that no changes or edits are made and the original work is properly cited (including links to both the formal publication through the relevant DOI and the license). See: <https://creativecommons.org/licenses/by-nc-nd/4.0/>.

References

- Zhang YA, Zhou Y, Luo X, et al. SHOX2 is a Potent Independent Biomarker to Predict Survival of WHO Grade II-III Diffuse Gliomas. *EBioMedicine* 2016;13:80-9.
- Cancer Genome Atlas Research Network; Brat DJ, Verhaak RG, et al. Comprehensive, Integrative Genomic Analysis of Diffuse Lower-Grade Gliomas. *N Engl J Med* 2015;372:2481-98.
- Hayes J, Yu Y, Jalbert LE, et al. Genomic analysis of the origins and evolution of multicentric diffuse lower-grade gliomas. *Neuro Oncol* 2018;20:632-41.
- Li M, Song X, Zhu J, et al. The interventional effect of new drugs combined with the Stupp protocol on glioblastoma: A network meta-analysis. *Clin Neurol Neurosurg* 2017;159:6-12.
- Li Y, Sharma A, Maciacyk J, et al. Recent Development in NKT-Based Immunotherapy of Glioblastoma: From Bench to Bedside. *Int J Mol Sci* 2022;23:1311.
- Walsh KM, Wiencke JK, Lachance DH, et al. Telomere maintenance and the etiology of adult glioma. *Neuro Oncol* 2015;17:1445-52.
- Bodnar AG, Ouellette M, Frolkis M, et al. Extension of life-span by introduction of telomerase into normal human cells. *Science* 1998;279:349-52.
- De Vitis M, Berardinelli F, Sgura A. Telomere Length Maintenance in Cancer: At the Crossroad between Telomerase and Alternative Lengthening of Telomeres (ALT). *Int J Mol Sci* 2018;19:606.
- Shay JW, Wright WE. Role of telomeres and telomerase in cancer. *Semin Cancer Biol* 2011;21:349-53.
- Bryan TM, Englezou A, Dalla-Pozza L, et al. Evidence for an alternative mechanism for maintaining telomere length in human tumors and tumor-derived cell lines. *Nat Med* 1997;3:1271-4.
- Gocha AR, Nuovo G, Iwenofu OH, et al. Human sarcomas are mosaic for telomerase-dependent and telomerase-independent telomere maintenance mechanisms: implications for telomere-based therapies. *Am J Pathol* 2013;182:41-8.
- Pezzolo A, Pistorio A, Gambini C, et al. Intratumoral diversity of telomere length in individual neuroblastoma tumors. *Oncotarget* 2015;6:7493-503.
- Arita H, Narita Y, Takami H, et al. TERT promoter mutations rather than methylation are the main mechanism for TERT upregulation in adult gliomas. *Acta Neuropathol* 2013;126:939-41.
- Lee DD, Leão R, Komosa M, et al. DNA hypermethylation within TERT promoter upregulates TERT expression in cancer. *J Clin Invest* 2019;129:223-9.
- Shay JW, Wright WE. Telomeres and telomerase: three decades of progress. *Nat Rev Genet* 2019;20:299-309.
- Pekmezci M, Rice T, Molinaro AM, et al. Adult infiltrating gliomas with WHO 2016 integrated diagnosis: additional prognostic roles of ATRX and TERT. *Acta Neuropathol* 2017;133:1001-16.
- Fan HC, Chen CM, Chi CS, et al. Targeting Telomerase and ATRX/DAXX Inducing Tumor Senescence and Apoptosis in the Malignant Glioma. *Int J Mol Sci* 2019;20:200.
- Braun DM, Chung I, Kepper N, et al. TelNet - a database for human and yeast genes involved in telomere maintenance. *BMC Genet* 2018;19:32.
- Kanehisa M, Goto S. KEGG: kyoto encyclopedia of genes and genomes. *Nucleic Acids Res* 2000;28:27-30.
- Yu G, Wang LG, Han Y, et al. clusterProfiler: an R package for comparing biological themes among gene clusters. *OMICS* 2012;16:284-7.
- Iasonos A, Schrag D, Raj GV, et al. How to build and interpret a nomogram for cancer prognosis. *J Clin Oncol* 2008;26:1364-70.
- Newman AM, Liu CL, Green MR, et al. Robust enumeration of cell subsets from tissue expression profiles. *Nat Methods* 2015;12:453-7.
- Chen R, Smith-Cohn M, Cohen AL, et al. Glioma Subclassifications and Their Clinical Significance. *Neurotherapeutics* 2017;14:284-97.
- Díez Valle R, Tejada Solís S, Idoate Gastearna MA, et al. Surgery guided by 5-aminolevulinic fluorescence in glioblastoma: volumetric analysis of extent of resection in single-center experience. *J Neurooncol* 2011;102:105-13.
- Eljamel S. 5-ALA Fluorescence Image Guided Resection of Glioblastoma Multiforme: A Meta-Analysis of the Literature. *Int J Mol Sci* 2015;16:10443-56.

26. Dongpo S, Zhengyao Z, Xiaozhuo L, et al. Efficacy and Safety of Bevacizumab Combined with Other Therapeutic Regimens for Treatment of Recurrent Glioblastoma: A Network Meta-analysis. *World Neurosurg* 2022;160:e61-79.
27. Louis DN, Perry A, Wesseling P, et al. The 2021 WHO Classification of Tumors of the Central Nervous System: a summary. *Neuro Oncol* 2021;23:1231-51.
28. Blasco MA. Telomeres and human disease: ageing, cancer and beyond. *Nat Rev Genet* 2005;6:611-22.
29. Dixit D, Prager BC, Gimble RC, et al. The RNA m6A Reader YTHDF2 Maintains Oncogene Expression and Is a Targetable Dependency in Glioblastoma Stem Cells. *Cancer Discov* 2021;11:480-99.
30. Zhang GH, Zhong QY, Gou XX, et al. Seven genes for the prognostic prediction in patients with glioma. *Clin Transl Oncol* 2019;21:1327-35.
31. Hopkins JL, Lan L, Zou L. DNA repair defects in cancer and therapeutic opportunities. *Genes Dev* 2022;36:278-93.
32. Yang F, Hu Z, Guo Z. Small-Molecule Inhibitors Targeting FEN1 for Cancer Therapy. *Biomolecules* 2022;12:1007.
33. Chen YD, Zhang X, Qiu XG, et al. Functional FEN1 genetic variants and haplotypes are associated with glioma risk. *J Neurooncol* 2013;111:145-51.
34. Sharma MC. Annexin A2 (ANX A2): An emerging biomarker and potential therapeutic target for aggressive cancers. *Int J Cancer* 2019;144:2074-81.
35. Huang Y, Jia M, Yang X, et al. Annexin A2: The diversity of pathological effects in tumorigenesis and immune response. *Int J Cancer* 2022;151:497-509.
36. Wang T, Wang Z, Niu R, et al. Crucial role of Anxa2 in cancer progression: highlights on its novel regulatory mechanism. *Cancer Biol Med* 2019;16:671-87.
37. Gonias SL, Zampieri C. Plasminogen Receptors in Human Malignancies: Effects on Prognosis and Feasibility as Targets for Drug Development. *Curr Drug Targets* 2020;21:647-56.
38. Ma K, Chen X, Liu W, et al. ANXA2 is correlated with the molecular features and clinical prognosis of glioma, and acts as a potential marker of immunosuppression. *Sci Rep* 2021;11:20839.
39. Bommhardt U, Schraven B, Simeoni L. Beyond TCR Signaling: Emerging Functions of Lck in Cancer and Immunotherapy. *Int J Mol Sci* 2019;20:3500.
40. Ge L, Xu L, Lu S, et al. LCK expression is a potential biomarker for distinguishing primary central nervous system lymphoma from glioblastoma multiforme. *FEBS Open Bio* 2020;10:904-11.
41. Zepecki JP, Snyder KM, Moreno MM, et al. Regulation of human glioma cell migration, tumor growth, and stemness gene expression using a Lck targeted inhibitor. *Oncogene* 2019;38:1734-50.
42. Kim RK, Yoon CH, Hyun KH, et al. Role of lymphocyte-specific protein tyrosine kinase (LCK) in the expansion of glioma-initiating cells by fractionated radiation. *Biochem Biophys Res Commun* 2010;402:631-6.

Cite this article as: Liu X, Wang J, Su D, Wang Q, Li M, Zuo Z, Han Q, Li X, Zhen F, Fan M, Chen T. Development and validation of a glioma prognostic model based on telomere-related genes and immune infiltration analysis. *Transl Cancer Res* 2024;13(7):3182-3199. doi: 10.21037/tcr-23-2294